Int. J. Ind. Chem. 2026; 17(1): 7-17

International Journal of Industrial Chemistry (IJIC)

https://doi.org/10.57647/IJIC.2026.1701.02

Research Article

A Super-Adsorbent Bis-Sulfonated Polyamide for Efficient Cobalt and Chromium Removal

Marzieh Iravani, Maryam Tayebani*

Department of Chemistry, Shah.C., Islamic Azad University, Shahreza, Iran

***Corresponding author:** tayebani47@iau.ac.ir

Article History:

Received:
3 January 2026

Revised:
30 February 2026

Accepted:
8 March 2026

Published in Issue:
31 March 2026

Abstract

Two aromatic polyamides containing sulfone and teraphthalaldehyde moieties were synthesized via the polycondensation reaction of bis-sulfonamide imine and bis-diaminodiphenylsulfone imine monomers with a diacyl chloride. The chemical structures and physicochemical properties of the synthesized polymers were comprehensively characterized by CHN analysis, ^{1}HNMR, FT-IR, UV–Vis spectroscopy, thermogravimetric/differential thermal analysis (TG/DTA), and scanning electron microscopy (SEM). The adsorption performance of the prepared polyamides toward Co^{2+} and Cr^{3+} ions in aqueous media was systematically investigated. The influence of key operational parameters, including pH, temperature, initial metal-ion concentration, and contact time, was evaluated to optimize adsorption efficiency. Under optimal conditions, the polymers exhibited remarkable removal efficiencies of 95.2% for Co^{2+} and 99% for Cr^{3+}. Metal ion concentrations before and after adsorption were quantified using atomic absorption spectrometry (AAS). Equilibrium data were analyzed using the Langmuir and Freundlich isotherm models, whereas adsorption kinetics were interpreted using pseudo-first-order and pseudo-second-order models to elucidate the mechanism governing metal-ion uptake.

Keywords: Polyamide, Adsorbent, Removal, Cobalt, Chromium, Heavy

Cite this article: Iravani & Tayebani, A Super-Adsorbent Bis-Sulfonated Polyamide for Efficient Cobalt and Chromium Removal. Int. J. Ind. Chem. 2026; 17(1): 7-17. https://doi.org/10.57647/IJIC.2026.1701.02

1. Introduction

Adsorbent materials for heavy metals such as Cr(III), Co(II), Cu(II), Hg(II), Pb(II), Cd(II), and Ni(II) are essential for every community since in almost all industrial processes producers face the production of heavy metal waste solutions that enter environmental cycles as pollutants [1, 2]. These pollutants have significant economic impacts (reducing the useful life of the instruments and pipes) and health effects (due to their toxicity, stability and biological interference with enzymes, proteins, nucleic acids) [3-5]. An effective method for heavy metal removal should be inexpensive, user friendly, simple and recyclable. Over the years, different techniques such as chemical precipitation [6], ion exchange [7], membrane filtration [8], chemical oxidation [9], reverse osmosis [10], solvent extraction [11], electrodialysis [12], ultrafiltration [13], and adsorption with activated carbon or hydrogel composites [14] have been used to remove heavy metals or other pollutants from aqueous solutions. Since these metals do not decompose easily, among the available methods, adsorption for heavy metal removal is the easiest and the most cost-effective method [16].

Cobalt is a heavy metal found in industrial effluents such as electroplating, alloy production, gas turbine production, and petrochemical industries, which can cause harmful side effects for humans in inorganic forms [15]. Cobalt is an essential element in the human body as in vitamin B12, but like other metals, excessive amounts are toxic and pose serious public health and environmental risks. Chronic cobalt poisoning can lead

to interstitial pneumonia, cardiac disorders, respiratory and skin sensitization, bone hyperplasia and polycythemia. It can also cause cardiomyopathy, hypothyroidism, neurological disorder, convulsions, blindness, headache, liver disease, and even cancer [16]. Chromium is one of the most problematic heavy metals because it exists in several oxidation states, mainly trivalent and hexavalent [17] Cr(III) is required in small amounts as micronutrients for glucose, fat, and protein metabolism in mammals, but large doses can be harmful to animals and plants [18]. Hexavalent chromium compounds with greater oxidation ability are far more toxic [19].

Synthesis of aromatic polyamides containing azomethine and sulfide groups has a great interest due to their high selectivity toward adsorption of heavy metal ions. Furthermore, according to the hard-soft-acid-base (HSAB) principle, ligands with N and S donor atoms can favorably adsorb heavy metals [20]. In fact, the lone pair electrons on nitrogen, sulfur, and oxygen of coordinating compounds act as potential active sites to form coordination complexes with heavy metal ions. Introducing heat-resistant groups such as aromatic rings into polyamide chains leads to their unusual properties such as hardness, thermal stability, and high tensile strength, physical, chemical, and mechanical resistance, as well as a high glass transition temperature [21, 22].

Therefore, to improve the chelating ability of new polymeric absorbents to heavy metals, many researchers aim to synthesize new polymeric adsorbents containing more heteroatoms in the polymer. The presence of azomethine group (C=N) units within the polymer structure increases the thermal stability as well as the complexation ability of the polymer [23-25]. Sulfur atoms in polymer structures, depending on the functional group type (such as thiourethane, monothio- or dithiocarbonates, thioesters, sulfinyls, sulfonyls, polysulfides, and sulfides), enhance the mechanical, electrical, optical and adhesive properties toward metals [26, 27]. As a result, it is very important to synthesize new polymer compounds with more heteroatoms to improve the chelating ability toward heavy metals.

In the present study, two aromatic polyamide polymers PL_1 and PL containing oxygen, nitrogen, and sulfur atoms in their backbone, were applied to the removal of heavy metals such as Co^{+2} and Cr^{+3} from aqueous solutions. The adsorption behaviors of these two metals under different metal concentrations, temperatures, reaction times, and pH values were investigated.

2. Experimental

2.1. Materials and Instruments

All chemical materials were of analytical grade. Sulfonamide (Merck), 4,4'-Diaminodiphenylsulfone (Merck), terephthalaldehyde (Sigma-Aldrich), terephthaloyl chloride (Merck), Ethanol (Merck,) HCl (Merck), pyridine (Py, Merck), N-Methyl-2-pyrrolidone (NMP, Merck). NMP was distilled under reduced pressure over calcium hydride (CaH_2) and was stored over 4Å molecular sieves before use. Dried lithium chloride (LiCl, Merck, at 200°C under vacuum) and dried calcium chloride ($CaCl_2$, Merck, at 250°C under under vacuum) were used. Infrared spectra were obtained by a Nicolet single beam FT-IR (400DImpact) spectrometer in the 400–4000 cm^{-1} range, using KBr disks at room temperature. Diffuse reflectance spectroscopy (DRS) was performed using a UV-Vis, model V-670, made in Japan. The ^{1}HNMR data were recorded by employing a Bruker AVANCE 400 MHz spectrometer. Elemental analyses were carried out by a Vario EL III Element Analyzer (Hanau, Germany). The crystalline structure was analyzed by diffractometer D8 ADVANCE from Bruker, Germany. Scanning electron microscopy (SEM) was used to investigate the morphology of the compounds (model MIRA3_LMU, made by TESCAN Company). Perkin Elmer Series elemental analyser was used for elemental analyses. TGA analysis was performed on a WRT-2P thermal analyzer (Shanghai Precision and Scientific Instrument, Shanghai, China) in ambient environment (N_2), from 25 up to 800°C by a linear heating rate of 10^0C min^{-1}. Ostwald viscometer (Germany) was used to measure inherent viscosity at 25 °C. FAAS, Perkin Elmer atomic absorption spectrometry was used to determine the ion content in the solution.

2.2. Monomer Synthesis L_1

L_1 ligand was prepared based on reported the procedure with slight changes in the synthesis method [28]. In a 100 mL round-bottomed flask (two-necked), 0.134 g (1 mmol) of terepthalaldehyde was added to 15 ml of dry acidic ethanol To the above mixture was combined with a suspension of 0.344 g (2 mmol) Sulfanilamide in 20 mL of ethanol (dry). The mixture was refluxed for 8-10 h in which the TLC was used to confirm the completion of the reaction. The solid product (cream colour) was separated, washed (ethanol) and dried (under vacuum at 70°C) (Scheme 1). (Yield is 89%). mp 260 °C (by DSC). ^{1}H NMR (400 MHz, DMSO): δ = 8.76 (s, 2H(a), -N=CH-), 8.13 (s, 4H(b), Ar-H), 7.89 (m, 4H(c), Ar-H), 7.46 (m, 4H(d), Ar-H), 7.40 (s, 4H(e), NH2). Elem. Anal. Calcd for $C_{20}H_{18}N_4S_2O_4$ (442.32 g/mol): C, 54.30%; H, 4.52%; N, 12.66%; S, 14.49%. Found: C, 54.42%; H, 4.09%; N, 12.89%; S, 14.79%. FT-IR. FTIR (KBr, cm^{-1}): 3178, 3307 (N–H), 1619 (C=N), 1486, 1408 (C=C), 1337(asymmetric) (S=O), 1156(symmetric) (S=O), (3037) (stretching frequency) (C-H) cm^{-1}.

10.57647/ijic.2026.1701.02

2.3. Polymer synthesis PL_1

The synthesis of PL_1 is as follows: To a 250 mL flask (three-necked) a mixture of 8 mL of dry NMP, 0.264 g (2.379 mmol) calcium chloride ($CaCl_2$) and 0.066 g (1.557 mmol) lithium chloride (LiCl) was added. To the obtained solution, 0.884 g (2 mmol) of L_1 was added and heated until all the salts had dissolved. Then 0.408 g (2.01 mmol) of terephthaloyl chloride was added slowly (within about 10 min) at -5 ºC to the above mixture and to the flask. When the mixture became well distributed, 0.5 mL of pyridine was added at high stirring speed. After stirring the reaction mixture at low temperature for another 20 min, the temperature was raised to room temperature for 3 h. Then, the flask was heated up to 45–50°C and the reaction was completed after 5h. Successively, the reaction mixture was cooled to room temperature, and then the mixture was poured into distilled water and filtered. The yellow solid was washed (water) and dried in a vacuum at 80◦C to a constant weight (product yield: 86.2%) (Scheme 1). mp 375 °C (by DSC). 1H NMR (400 MHz, DMSO): δ= 10.78, 10.81 (s, H, -HN-C=O), 8.11 (s, 2H, -N=CH-), 8.05 (d, 4H, Ar-H), 7.97 (d, 4H Ar-H), 7.85 (d, 4H, Ar-H), 7.53 (d, 4H, Ar-H). Elem. Anal. Calcd. for $(C_{28}H_{20}N_4S_2O_6)_n$ $(572.4\ g/mol)_n$: C, 58.75%; H, 4.89%; N, 9.78%; S, 11.20%. Found: C, 59.05%; H, 5.20%; N, 9.90%; S, 11.55%. FT-IR (KBr, cm^{-1}): 3356, 3311 (NH), 1597 (C=N), 1533 (C=C), 1532 (asymmetric) (S=O), 1155 (symmetric) (S=O). 1668 (C=O), 1401 (amide) (C-N) cm^{-1}.

2.4. Monomer and Polymer synthesis L , PL

The monomer L and PL were synthesized according to the previously reported procedures, following the exact method described [29] (Scheme 2)

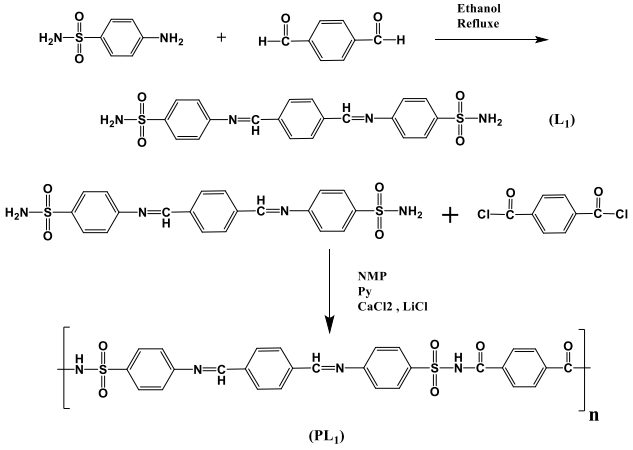

Scheme 1. Synthesis of monomer L_1 and polyamide PL_1

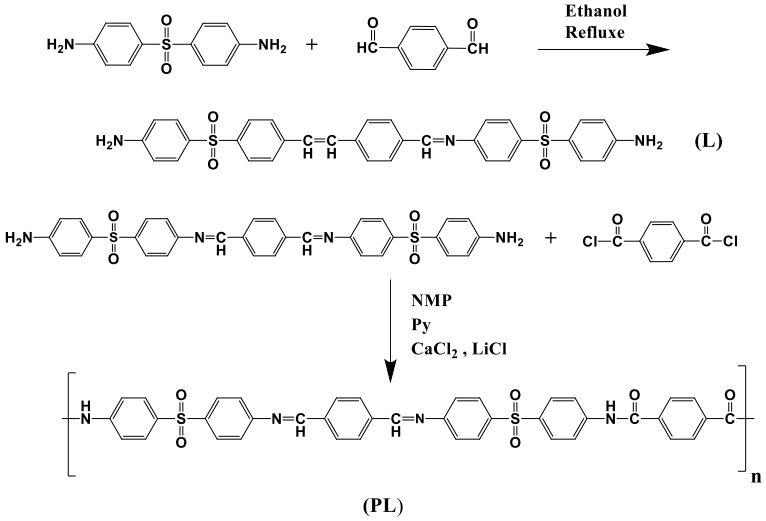

Scheme 2. Synthesis of monomer L and polyamide PL

10.57647/ijic.2026.1701.02

2.5. Metal Ion Adsorption Studies

The batch equilibrium method was employed to investigate the removal of Co(II) and Cr(III) ions by Poly(azomethine amides PL_1 and PL in aqueous solutions. The dilute solutions of HCl/NaOH were used to keep the pH constant. Separately, 2 mg of PL_1 and PL adsorbents were added to 50 mL of metal ion ($CoCl_2{\cdot}6H_2O$, $CrCl_3{\cdot}6H_2O$) solutions (20 ppm) and were stirred for 2 h at 200 rpm to facilitate the adsorption of cobalt and chromium on the polymers. To determine the ion content in the solution, atomic absorptionn spectrometry was used.

The variables considered in this study were: pH (3-8), metal-ion concentration (10–35 ppm), temperature (30–60 °C), and time (20–120 min). The removal efficiency (R%) of the metal ions was calculated by the using Eq. (1):

$$R\% = \frac{C_0 - C_e}{C_0} \times 100 \quad (1)$$

C_0: the initial concentrations of the metal ion (mg L^{-1})
C_e: equilibrium concentrations of the metal ion (mg L^{-1})

3. Result and discussion

3.1. FT-IR spectra

The characteristic absorption bands of amine groups of Schiff base (L_1) and its corresponding polyamide (PL_1) were observed in 3178-3356 cm^{-1}. The vibrational frequency of the azomethine group (–N=CH–) appeared at 1597-1619 cm^{-1} and the symmetric and asymmetric vibrations of the sulfone group (SO_2) were found at 1155-1532 cm^{-1}. The polymer also exhibited a characteristic absorption band of amid group (O=C) at 1668 cm^{-1} (Fig. 1a) [30-33].

3.2. ^{1}H NMR spectroscopy

The ^{1}H NMR spectra of all synthesized compounds were consistent with the proposed structures. The signals corresponding to azomethine protons in the monomer L_1 and polyamide PL_1 appeared at δ= 8.76 and 8.11 ppm respectively. The N–H proton signals of PL_1 appeared at 10.75 and 10.81 corresponding to probable different conformations of cis and trans isomers, indicating the presence of amide groups in the main chain. [34] The resonance signal around 7.40 ppm was assigned to the NH_2 group of Schiff base ligand (L_1) which was absent in PL_1. The aromatic proton occurs in the range of 7.46-8.13 ppm for both monomer and its corresponding polymer [35, 36].

3.3. Electronic spectra

The electronic spectra of monomer L_1 and the corresponding polymer were recorded using UV-Visible spectroscopy in ethanol solvent (Fig. 1b). In the spectrum of the monomer transitions of ($\pi \rightarrow \pi^*$) of both the aromatic ring and the azomethine group were observed around 260 and 340 which were shifted to the higher energy region for the polymer [36, 37].

3.4. Surface morphology studies

The morphological features of polyamide PL_1 and its corresponding metal-loaded samples were investigated by scanning electron microscopy (SEM). As illustrated in Fig. 2, PL_1 exhibits a sponge-like, homogeneous, and porous surface morphology, characterized by the presence of nanoparticles or nanospheres typically observed in polyamides precipitated from solution. The morphology of PL_1 is highly comparable to that of PL, indicating similar surface and textural properties. This structural similarity suggests that both polymers are promising candidates for the adsorption of heavy metal ions from contaminated aqueous media. Following exposure to metal ion solutions, significant morphological transformations were observed. The polymer surface underwent marked structural rearrangement, exhibiting a plate-like morphology in the presence of Cr^{3+} ions and a predominantly spherical morphology after Co^{2+} adsorption. These morphological changes can be attributed to the coordination and subsequent deposition of metal ions onto the functional groups of the polymer matrix. PL can therefore be considered a nanostructured adsorbent. The noticeable variation in surface texture at the ~300 nm scale between the pristine sample (a) and the metal-loaded samples (c–f) confirms the interaction of Co^{2+} and Cr^{3+} ions with the polymer at the nanoscale, leading to the formation of nanoscale metal-associated domains on the surface. These findings provide further evidence of the high adsorption capability of the synthesized polyamides for metal ion removal [2, 27, 29, 36].

3.5. X-ray diffraction analysis

The XRD pattern of PL_1, reveals its semi-crystalline nature The diffractogram exhibits several well-defined peaks distributed over a broad angular range (5°–75° 2θ), indicating the coexistence of ordered and disordered domains within the polymer matrix. In polymer systems, the appearance of distinct diffraction maxima signifies the presence of crystalline regions embedded in an amorphous matrix. The diffraction peak at 5.03° (2θ) shows relatively high intensity. Although low-angle reflections in polymers are sometimes associated with

10.57647/ijic.2026.1701.02

interchain spacing or partially ordered amorphous domains, the pronounced intensity of this peak suggests the presence of a periodic structural arrangement. The most intense diffraction peak (100% relative intensity) is observed at 20.0° (2θ), which can be attributed to the principal crystallographic plane of the polymer lattice. Additional reflections appear at 15.0° (25% relative intensity), 25.0° (25%), and 30.0° (18%) (2θ), corresponding to secondary crystalline planes within the unit cell structure [20, 29, 33, 38]. Overall, the XRD results confirm that PL_1 possesses a semi-crystalline morphology characterized by well-defined crystalline domains dispersed within an amorphous polymer matrix.

3.6. Thermogravimetric analysis

The TGA method was applied to assess the thermal stability of the polyimines. This analysis can evaluate the thermal stability and degradation behavior related to the sample. The TGA and DTG curves of PL_1 are shown in (Fig. 1d) In the TGA curve of the polymer an insignificant weight loss (about 5-10%) from 116ºC to 300ºC can be attributed to solvent evaporation. A mass loss of about 40% is observed between 350 ºC and 450 ºC for PL_1 indicating the high stability of the synthesized polymers at high temperatures and their resistance to decomposition at that temperature. PL_1 retained 30% of its initial weight upon heating to 600 °C, demonstrating its high thermal stability. In the DTG curve, a sharp endothermic peak can be observed around 350ºC for PL_1 with a loss weight rate of 9% min^{-1}, ascribed to the decomposition and char formation of PL_1 [34, 39]. The TGA results confirm the excellent thermal performance of this polymer which is comparable with PL [29].

4. Application of polyamides PL_1 and PL_2 for removing Cr and Co:

4.1. Effect of pH

For both polymers, with a contact time of 2 h, an M(II) concentration of 20 ppm, and 2 mg of polyamide at 25°C, the pH values were adjusted from 3 to 8. The optimum pH for adsorption capacities of the PL_1 and PL for Co(II) and Cr(III) was found to be 7. It seems that, due to protonation of the binding sites of ligands at low pH, there will be less coordination with metal ions, resulting in minimal M(II) removal.

4.2. Initial concentration effect

The adsorption capacities of polyamides PL_1 and PL were evaluated in the M(II) concentration range of 10-35 mg/L, with other parameters kept constant (pH=7, contact time=2 h and room temperature). As shown in Fig. 3b and 4b, the removal percentage decreased with increasing Co(II) and Cr(III) concentration. For PL and Co(II), the removal percentage decreased from 98.33 % to 54.57% as the concentration increased from 15 to 35 mg/L. For Cr(III) and PL, the decrease in the removal percentage was smaller (from 100 to 74.22%) under the same condition. For Cr(III) even a concentration of 20 mg/L resulted in a satisfactory removal of 10 mg/L.

Therefore, the optimal concentration values for removal are 15 mg/L for Co(II) and 20 mg/L for Cr(III). The diminishing trend observed with increasing metal(II) concentration can be attributed to the saturation of the coordination sites of the polyamides, which reduces metal adsorption and consequently lowers the efficiency of the adsorbent.

4.3. Temperature effect

The temperature was varied from 25-60°C to investigate the removal of Cr(III) and Co(II) by PL_1 and (at pH= 7, contact time of 2 h, and the M(II) concentration of 20 ppm, with 2 mg of polyamide,). As shown in Fig. 3c and 4c for both polyamide (PL_1 and PL) and both metal ions (Co(II) and Cr(III)), the removal percentage decreases when the temperature increases from 30 to 40°C. However, from 40-60°C, the removal percentage increases, consistent with an endothermic adsorption process, as it has been reported in other cases of endothermic heavy-metal adsorption [37]. The behaviour of the polymers for different metal [2]. ions follows the same trend, with polyamide PL demonstrating superior adsorption performance at 60°C.

4.4 Effect of time

Another important factor influencing the removal percentage is contact time. Time intervals of 20, 40, 60, 80, 100, 120, and 140 minutes were considered to investigate the removal efficiency of Co(II) and Cr(III), while maintaining other parameters at their optimum values (pH = 7, M(II) concentration = 20 ppm, polyamide dosage = 2 mg, and temperature = 25°C) (Fig. 3d and Fig. 4d).

With increasing contact time, the removal percentage varied for the two polyamides with different metals. For Co(II), PL achieved the highest removal efficiency at 80 min (95.20%), while PL_1 reached its maximum at 100 min (89.15%). For Cr (III), PL_1 exhibited maximum removal at 100 min (96.65%), whereas PL achieved its highest efficiency at 120 min (99%). These results indicate that both polyamides possess a high capacity for metal removal. As contact time increases, saturation of the coordination sites of the polymer occurs, leading to equilibrium in adsorption. From Fig. 3, the optimum conditions for Co(II) removal with PL are: pH = 7, initial concentration 15 mg/L, temperature 30°C, and contact

10.57647/ijic.2026.1701.02

time 80 min. For PL_1, the optimum conditions are: pH = 7, initial concentration 15 mg/L, temperature 30°C, and contact time 100 min.

As demonstrated in Fig.4 for Cr(III) and PL : pH=7, an initial concentration 20 mg/L, temperature 60°C and time 120 min, and for PL_1: pH=7, Initial concentration 10 mg/L, temperature 60°C and time 100 min are the optimum conditions (Fig. 4).

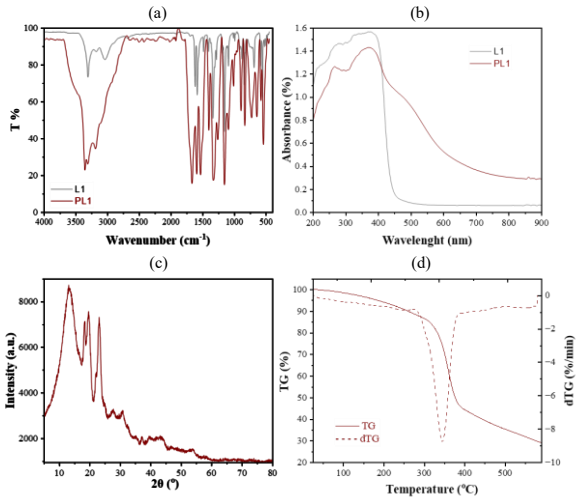

Figure 1. (a) The FT-IR spectrum of the L_1 and PL_1, (b) The UV-Vis spectrum of L_1 and PL_1, (c) X-ray diffraction patterns of: PL_1, (d) TGA and DTG curves of PL_1

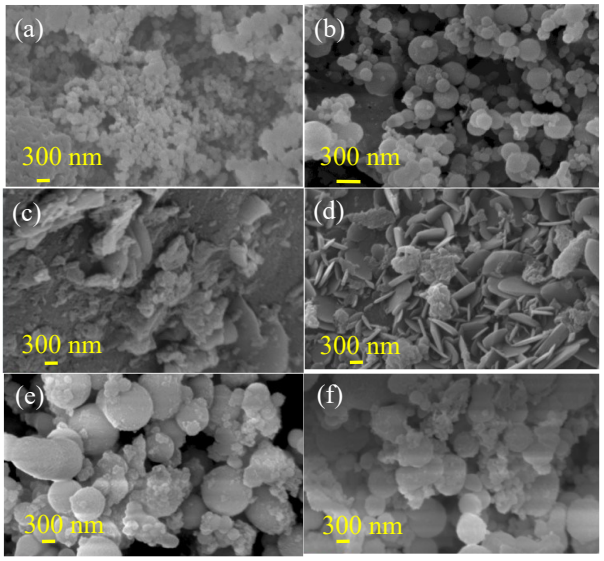

Figure 2. SEM images of: (a) PL_1 (b) PL (C) absorbed PL_1/Co d) absorbed PL_1/Cr e) absorbed PL/Co f) absorbed PL/Cr

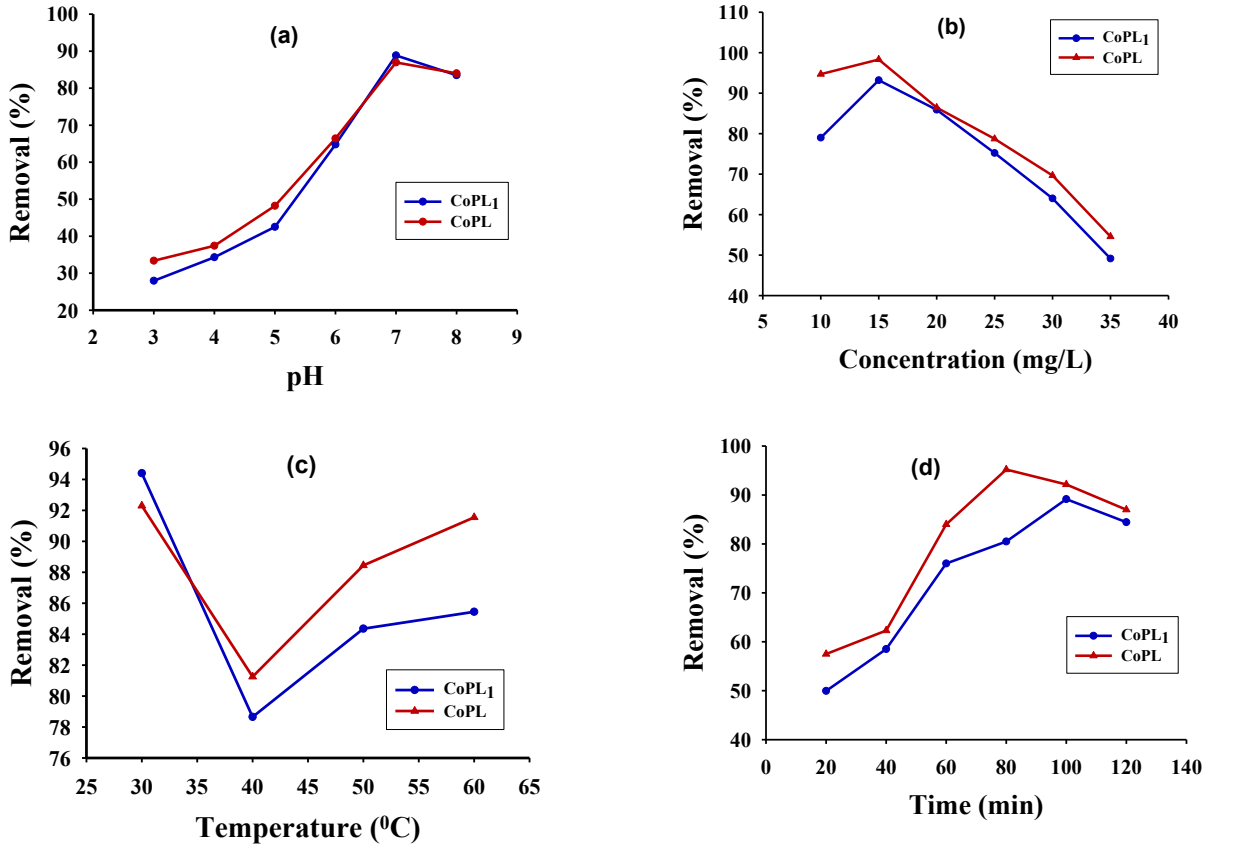

Figure 3. The effect of (a) pH (3- 8), (b) concentration (10–35 mg/L), (c) temperature (30–60ºC) and (d) contact time (30–120 min) on adsorption of Co(II) by the polymer

10.57647/ijic.2026.1701.02

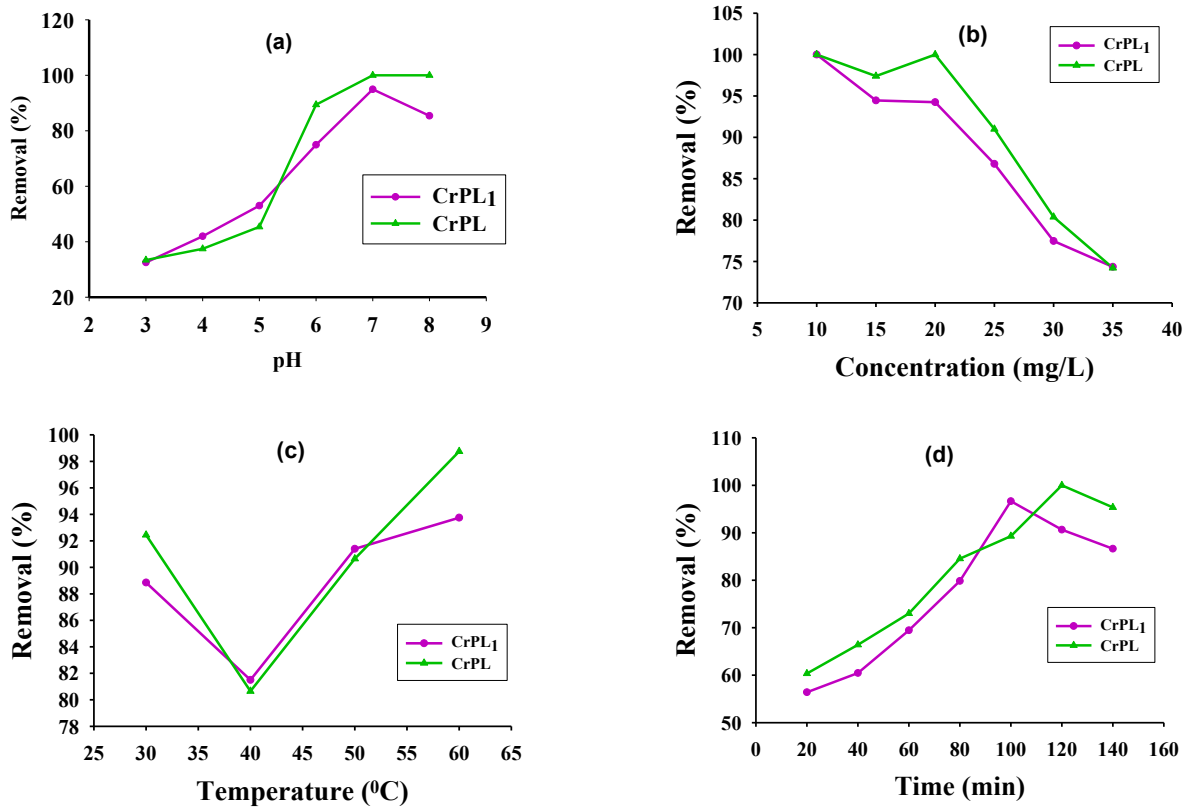

Figure 4. The effect of (a) pH (3- 8), (b) concentration (10–35 mg/L), (c) temperature (30–60◦C) and (d) contact time (30–140 min) on adsorption of Cr(III) by the polymer PL1 and PL

4.5 Adsorption Isotherms

To describe the interaction of metals with the adsorbent, two models have been considered: The first one is the Langmuir model which assumes that adsorption occurs in a homogeneous medium without molecular interactions [40]. The Langmuir equation (Equation 2) describes adsorption as a monolayer process on the adsorbent surface:

$$\frac{C_e}{q_e} = \frac{1}{q_{max} K_L} + \frac{1}{q_{max}} C_e \qquad (2)$$

Ce: the metal concentration mg L^{-1}
kL: Langmuir constant L mg^{-1}
qmax: maximum monolayer adsorption capacity mg g^{-1}
qe: the amount of metal adsorbed per gram of polymer at equilibrium mg g^{-1})

In this model, the Langmuir constant (K_L) and q_{max} is maximum adsorption capacity (which is calculated from the slope and intercept of the linear plot of C_e/q_e vs. C_e) (Fig. 5a, Table 1)

The second model is the Freundlich which is based on a multilayer adsorption surface and is represented by equation (3):

$$\log q_e = \log k_f + \frac{1}{n} \log C_e \qquad (3)$$

1/n: Freundlich constant (related to adsorption intensity/strength)
K_f: multilayer adsorption capacity

The values of K_f and 1/n were determined from the intercept and slope, respectively, of the linear plot of log q_e versus log C_e (Fig. 5b and Table 1).

The Langmuir model exhibited excellent agreement with the experimental data, with correlation coefficients (R^2) ranging from 0.9664 to 0.9971. Among the investigated adsorbents, $CrPL_1$ and CrPL exhibited higher adsorption capacities toward Cr(III) ions, indicating their superior adsorption performance. The relatively high K_L values further demonstrate the strong affinity of the synthesized polyamides toward the investigated metal ions (Table 1). The Freundlich model also adequately described the adsorption equilibrium. The calculated K_F values confirming the high adsorption capacity of the prepared polymers. Since all the Freundlich exponent (n) values are greater than 1, the adsorption process can be considered favourable, indicating strong interactions between the adsorbent surface and the metal ions.

Overall, both isotherm models satisfactorily described the adsorption process; nevertheless, the higher R^2 values

10.57647/ijic.2026.1701.02

obtained from the Langmuir model indicate that monolayer adsorption predominates for the adsorption of Co(II) and Cr(III) onto the synthesized polyamides. The adsorption of Co(II) and Cr(III) by the synthesized polyamides is mainly governed by coordination interactions between the metal ions and the nitrogen- and oxygen-containing functional groups, including amide, sulfone, and azomethine groups. The aromatic rings may also contribute through electron-rich π systems. The Langmuir model generally exhibited higher correlation coefficients than the Freundlich model, indicating that adsorption predominantly occurs on relatively homogeneous active sites with monolayer surface coverage. The differences observed between Co(II) and Cr(III) adsorption can be attributed to their different ionic radii, charge densities, and coordination preferences, which influence their interactions with the available functional groups of the polymers.

4.6 Kinetics Study

The rate and mechanisms that govern metal adsorption are described by adsorption Kinetics pseudo first order (PFO) and the pseudo second order (PSO) and are presented by equations (4) and (5) respectively [41]

$$\ln(q_e - q_t) = \ln q_e - k_1(t) \quad (4)$$

$$\frac{t}{q_t} = \frac{1}{k_2 q_e^2} + \frac{t}{q_e} \quad (5)$$

q_e: adsorption capacity (at equilibrium mg/g)
q_t: adsorption capacity (at time t mg/g)
k_1: rate constant the pseudo first order min^{-1}
k_2: rate constant of the pseudo second order $gmg^{-1}min^{-1}$
t: time min

The intercept and slope of the linear plot of $\ln(qe - q_t)$ vs. t provide the amount of k_1 and qe in the Pseudo-First-Order (PFO) model (Fig. 6a, Table 2). In the Pseudo-Second-Order (PSO) model, the K_2 and q_e values are obtained from the intercept and slope of the linear plot of t/qt versus t (Fig. 6b). The high correlation coefficients (R^2 = 0.9640-0.9817) indicate that metal adsorption follows the PSO model for Co(II) and Cr(III) removal. This suggests that the adsorption process occurred predominantly through chemical interaction between the metal ions and the active sites on polymers surface, represented the two phase system. The pseudo-second-order model implies the chemical interactions between metal ions and the adsorbents and are the rate limiting step for metal ions removal from water solutions.

Table 1: Parameters of Langmuir and Freundlich isotherm constants for adsorption of Co(II) and Cr(III)

	Langmuir			Freundlich		
Absorbent	q_{max} (mg g^{-1})	K_L (Lmg^{-1})	R^2	K_f((mg g^{-1})(L mg^{-1})$^{1/n}$)	n	R^2
$CoPL_1$	468.51	1.2506	0.9664	291.13	5.7174	0.3117
CoPL	495.69	4.8311	0.9954	359.06	7.2936	0.5836
$CrPL_1$	654.34	2.1925	0.9903	409.16	4.8039	0.8764
CrPL	646.09	6.1107	0.9971	448.97	5.5367	0.9460

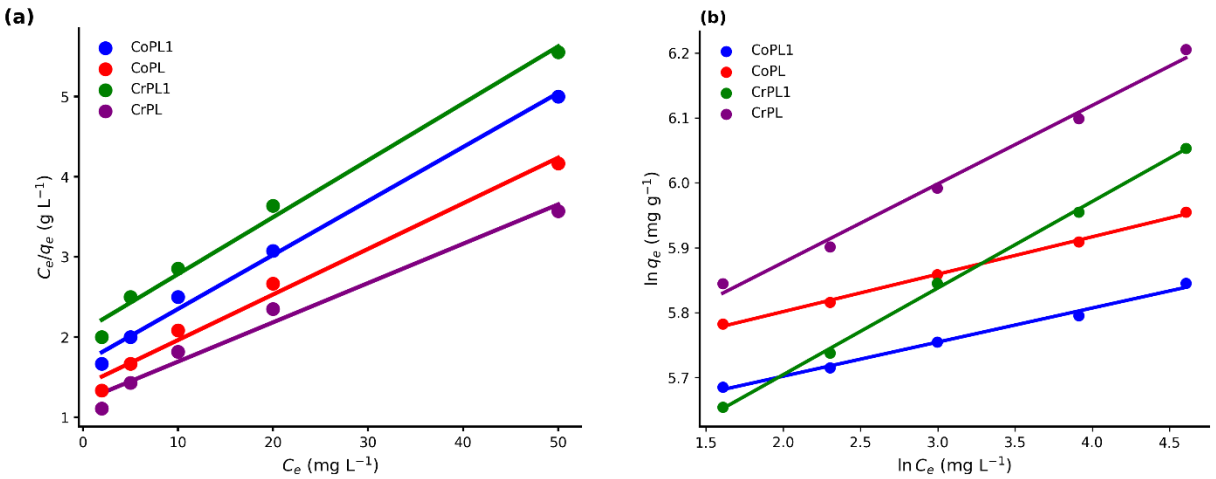

Fig. 5: a) Langmuir isotherm b) Frenundlich isotherm of PL_1 and PL metal complexes

5. Conclusions

The two new polyamides were successfully applied for the removal of Co(II) and Cr(III) metal ions from aqueous solutions. Optimized conditions for adsorption were established based on contact time, temperature, pH, and initial concentration. The adsorption kinetics of both metal ions followed the pseudo-second-order model, indicating that chemical interactions between the metal ions and the active sites of the polymers are the rate-limiting step. The most appropriate adsorption isotherm model varied depending on the adsorbent and the specific metal ion, although the R^2 values for both models were very close, suggesting good applicability of both. The two polyamides superior adsorption performance compared to PL_1, and the removal efficiency was higher for Cr(III) than for Co(II). These findings highlight the potential of poly(azomethine amides) as effective adsorbents for the treatment of heavy-metal-contaminated water.

Table 2: Adsorption kinetic data for removal of Co(II) and Cr(III)

Compound	$qe_{(exp.)}$(mg g^{-1})	$qe_{(calc.)}$(PFO)	K_1(PFO)	R^2(PFO)	$qe_{(calc.)}$(PSO)	K_2(PSO)	R^2(PSO)
$CoPL_1$	445.75	304.434	0.0224	0.9609	528.626	7.47e-05	0.9817
CoPL	476.00	272.267	0.0213	0.7179	529.271	1.03e-04	0.9640
$CrPL_1$	483.25	296.510	0.0152	0.8675	530.491	7.88e-05	0.9644
CrPL	500.00	339.725	0.0186	0.9779	570.997	6.77e-05	0.9801

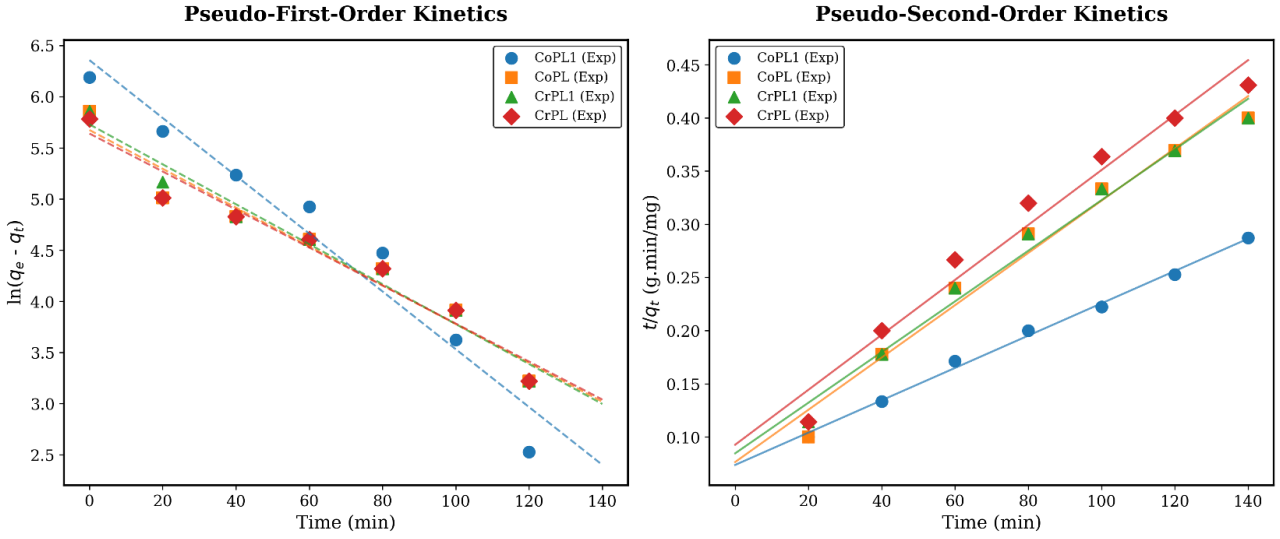

Fig. 6: Linear plots of Pseudo-first-order kinetic and Pseudo-second-order kinetic model for the adsorption of Co(II) and Cr(III) onto PL and PL_1

Acknowledgements

The authors gratefully acknowledge the Islamic Azad University of Shahreza for institutional support.

Authors' Contribution

All the authors have participated sufficiently in the intellectual content, conception, and design of this work or the analysis and interpretation of the data (when applicable), as well as the writing of the manuscript.

Availability of data and materials

The data that support the findings of this study are available from the corresponding author upon reasonable. request.

Conflict of interest

The author states that there is no conflict of interest

10.57647/ijic.2026.1701.02

References

[1] Narwade VN, Khairnar RS, Kokol V. In situ synthesized hydroxyapatite-cellulose nanofibrils as biosorbents for heavy metal ions removal. J Polym Environ. 2018;26:2130-2141. https://doi.org/10.1007/s10924-017-1101-7

[2] Aghaei M, Kianfar AH, Dinari M. Synthesis and characterization of a novel Schiff base polyamide ligand and its copper(II) complex for comparative removal of Pb(II) ions from aqueous solutions. J Polym Res. 2020;27:1-13. https://doi.org/10.1007/s10965-020-2007-y

[3] Jaishankar M , Tseten T, Anbalagan N, Mathew BB, Beeregowda KN. Toxicity, mechanism and health effects of some heavy metals. Interdiscip Toxicol. 2014;7:60-72. https://doi.org/10.2478/intox-2014-0009

[4] Qureshi F, Memon SQ, Khuhawar MY, Jahangir TM. Removal of Co^{2+}, Cu^{2+} and Au^{3+} ions from contaminated wastewater by using new fluorescent and antibacterial polymer as sorbent. Polym Bull. 2021;78:1505-1533. https://doi.org/10.1007/s00289-020-03170-y

[5] Kadim MK, Risjani Y. Biomarker for monitoring heavy metal pollution in aquatic environment: an overview toward molecular perspectives. Emerg Contam. 2022;8:195-205. https://doi.org/10.1016/j.emcon.2022.02.003

[6] Peng H, Guo J, Li B, Huang H, Shi W, Liu Z. Removal and recovery of vanadium from waste by chemical precipitation, adsorption, solvent extraction, remediation, photo-catalyst reduction and membrane filtration: a review. Environ Chem Lett. 2022;20:1763-1776. https://doi.org/10.1007/s10311-022-01395-z

[7] Kaith BS. Removal of hazardous metal ions from polluted water using biomaterial-based ion-exchangers: a review. Mater Today Proc. 2022;53:174-187. https://doi.org/10.1016/j.matpr.2021.12.495

[8] Xiang H, Min X, Tang CJ, Sillanpää M, Zhao F. Recent advances in membrane filtration for heavy metal removal from wastewater: a mini review. J Water Process Eng. 2022;49:103023. https://doi.org/10.1016/j.jwpe.2022.103023

[9] Haripriyan U, Gopinath KP, Arun J. Chitosan based nano adsorbents and its types for heavy metal removal: a mini review. Mater Lett. 2022;312:131670. https://doi.org/10.1016/j.matlet.2022.131670

[10] Haro-Martínez A, Arroyo-Carrasco R, Galván L, Sayago A, Cuadri AA, Martín-Alfonso JE, et al. Competitive and synergistic effects of metal adsorption in water remediation processes mediated by hybrid copolymers. Chem Eng J. 2023;470:143905. https://doi.org/10.1016/j.cej.2023.143905

[11] Pavón S, Haneklaus N, Meerbach K, Bertau M. Iron(III) removal and rare earth element recovery from a synthetic wet phosphoric acid solution using solvent extraction. Miner Eng. 2022;182:107569. https://doi.org/10.1016/j.mineng.2022.107569

[12] Cerrillo-Gonzalez MM, Villen-Guzman M, Rodriguez-Maroto JM, Paz-Garcia JM. Metal recovery from wastewater using electrodialysis separation. Metals. 2024;14(1):38. ttps://doi.org/10.3390/met14010038

[13] Wang Y, Li D, Li J, Fan M, Han M, Liu Z, et al. Metal organic framework UiO-66 incorporated ultrafiltration membranes for simultaneous natural organic matter and heavy metal ions removal. Environ Res. 2022;208:112651. https://doi.org/10.1016/j.envres.2021.112651

[14] Abdeli H, Sazegar MR, Kabirifard H, Asnaashari-Isfahani M. Synthesis of composites based on PVA/Chitosan/Fe or Zn@Itaconic acid: investigation of itaconic acid concentrations to remove organic dye pollution. Int J Ind Chem. 2025;16:162501. https://doi.org/10.57647/j.ijic.2025.1601.01

[15] Kosiorek M, Wyszkowski M. Effect of cobalt on the environment and living organisms: a review. Appl Ecol Environ Res. 2019;17:11419-11449. https://dx.doi.org/10.15666/aeer/1705_1141911449

[16] Czarnek K, Terpiłowska S, Siwicki AK. Selected aspects of the action of cobalt ions in the human body. Cent Eur J Immunol. 2015;40:236-242. https://doi.org/10.5114/ceji.2015.52837

[17] Prasad S, Yadav KK, Kumar S, Gupta N, Cabral-Pinto MMS, Rezania S, et al. Chromium contamination and effect on environmental health and its remediation: a sustainable approach. J Environ Manage. 2021;285:112174. https://doi.org/10.1016/j.jenvman.2021.112174

[18] Saeed AA, Sandhu MA, Khilji MS, Yousaf MS, Rehman HU, Tanvir ZI, Ahmad T. Effects of dietary chromium supplementation on muscle and bone mineral interaction in broiler chicken. J Trace Elem Med Biol. 2017;42:25-29. https://doi.org/10.1016/j.jtemb.2017.03.007

[19] Chaâbane M, Bejaoui S, Trabelsi W, Telahigue K, Chetoui I, Chalgha M, et al. The potential toxic effects of hexavalent chromium on oxidative stress biomarkers and fatty acids profile in soft tissues of Venus verrucose. Ecotoxicol Environ Saf. 2020;196:110562. https://doi.org/10.1016/j.ecoenv.2020.110562

[20] Sayed MM, Abdel-Hakim M, Mahross MH, Aly KI. Synthesis, physico-chemical characterization, and environmental applications of mesoporous crosslinked poly(azomethine-sulfone)s. Sci Rep. 2022;12:12878 https://doi.org/10.1038/s41598-022-17042-0

[21] Sikkema DJ. Chapter 4: Rigid-chain polymers: Aromatic polyamides, heterocyclic rigid rod polymers, and polyesters. Adv Ind Eng Polym Res. 2022;5:80-89. https://doi.org/10.1016/j.aiepr.2022.03.003

[22] Hernández G, Ferrero S, Reinecke H, Bartolomé C, Martinez-Ilarduya JM, Álvarez C, et al. New insights in the synthesis of high-molecular-weight aromatic polyamides—improved synthesis of rod-like PPTA. Int J Mol Sci. 2023;24:2734. https://doi.org/10.3390/ijms24032734

[23] Nozha SG, Morgan SHM, Abu Ahmed SE, El-Mogazy MA, Diab MA, El-Sonbati AZ, et al. Polymer complexes. LXXIV. Synthesis, characterization and antimicrobial activity studies of polymer complexes of some transition metals with bis-bidentate Schiff base. J Mol Struct. 2021;1227:129525. https://doi.org/10.1016/j.molstruc.2020.129525

[24] Ahmad M, Manzoor K, Ahmed S, Ikram S. Synthesis and characterization of terephthalaldehyde–thiocarbohydrazide polymer doped with Cu(II) and Zn(II) metal ions for solar cell applications. Optik. 2016;127:4329-4332. https://doi.org/10.1016/j.ijleo.2016.01.199

[25] Mighan HJ. Schiff Base polymers: synthesis and characterization. Polym Res. 2020;27:1-18. https://doi.org/10.1007/s10965-020-02080-x

[26] Javadi A, Shockravi A, Koohgard M, Malek A, Shourkaei F, Ando S. Nitro-substituted polyamides: a new class of transparent and highly refractive materials. Eur Polym J. 2015;66:328-341. https://doi.org/10.1016/j.eurpolymj.2025.02.032

[27] Rezania H, Vatanpour V, Salehi E, Gavari N, Shockravi A, Ehsani M. Wholly heterocycles-based polyamide–sulfide containing pyridine and thiazole rings: a super-adsorbent polymer for lead removal. J Polym Environ. 2019;27:1790-1800. https://doi.org/10.1007/s10924-019-01473-4

[28] Akocak S, Lolak N, Nocentini A, Karakoc G, Tufan A, Supuran CT. Synthesis and biological evaluation of novel aromatic and heterocyclic bis-sulfonamide Schiff bases as carbonic anhydrase I, II, VII and IX inhibitors. Bioorg Med Chem. 2017;25:3093-3097. https://doi.org/10.1016/j.bmc.2017.03.063

[29] Iravani M, Tayebani M. Band gap studies on a thermally stable polyimine polymer and its metal complexes. ChemistrySelect. 2024;9:e202401054. https://doi.org/10.1002/slct.202401054

[30] Ebrahimi H, Hadi JS, Al-Ansari HS. A new series of Schiff bases derived from sulfa drugs and indole-3-carboxaldehyde: synthesis, characterization, spectral and DFT computational studies. J Mol Struct. 2013;1039:37-45. https://doi.org/10.1016/j.molstruc.2013.01.063

[31] Ravikumar L, Saravanan R. Synthesis of soluble, curable, and thermally stable aromatic polyamides bearing thiourea and pendent 4-pyridylformylimino groups. Int J Polym Mater. 2012;61:1050-1064. https://doi.org/10.1080/00914037.2011.617335

[32] Abdel-Rahman MA, El-Said WA, Sayed EM, Abdel-Wahab AMA. Synthesis, characterization of some conductive aromatic polyamides/Fe_3O_4 NPs/ITO, and their utilization for methotrexate sensing. Surfaces. 2023;6:83-96. https://doi.org/10.3390/surfaces6010007

[33] Jia L, Wang D, Liu L, Zhang S, Xu T. Preparation of novel poly(amide-sulfonamide) (PASA) and its application in 2,4-dinitrophenol adsorption. Des Monomers Polym. 2014;17:425-429. https://doi.org/10.1080/15685551.2013.867565

[34] Abraham RJ, Griffiths L, Perezc M. 1H NMR spectra part 31: ^{1}H chemical shifts of amides in DMSO solvent. Magn Reson Chem. 2014;52:395-408. https://doi.org/10.1002/mrc.4079

[35] Li Z, Zhang G, Li D, Yang J. Polyamides containing thiadiazole units: synthesis and optical properties. Chin J Polym Sci. 2014;32:292-304. https://doi.org/10.1007/s10118-014-1407-z

[36] Qureshi F, Khuhawar MY, Jahangir TM, Channar AH. Synthesis and characterization of new thermally stable, antimicrobial and red-light-emitting poly(azomethine-ester)s. Polym Bull. 2021;78:5055-5074. https://doi.org/10.1007/s00289-020-03357-3

[37] Gao B, Zhang D, Li Y. Synthesis and photoluminescence properties of novel Schiff base type polymer-rare earth complexes containing furfural-based bidentate Schiff base ligands. Opt Mater. 2018;77:77-86. https://doi.org/10.1016/j.optmat.2017.12.052

[38] Balasubramaniam B, Selvaraj A, Iyer NR, Ravikumar L, Rai PK, Mondal K, et al. Electrochemical and microstructural analysis of azomethine polyamides as inhibitor for rebar corrosion under chloride contaminated pore solution. Frontier Res Today. 2018;1:11-10. https://doi.org/10.31716/frt.201801004

[39] Faghihi K, Naderi-Ghomi M, Hajibeygi M. Synthesis and properties of new polyamide-organoclay nanocomposites containing pyrazine moiety in the main chain. Sci Eng Compos Mater. 2012;19:215-220. https://doi.org/10.1515/secm-2011-0105

[40] McKay G. The adsorption of basic dye onto silica from aqueous solution-solid diffusion model. Chem Eng Sci. 1984;39:129-138. https://doi.org/10.1016/0009-2509(84)80138-4

[41] Ho Y, McKay G. Pseudo-second order model for sorption processes. Process Biochem. 1999;34:451-465. https://doi.org/10.1016/S0032-9592(98)00112-5